A molecular simulation study of a cyclic siloxane with attached biphehylyl 4-allyloxybenzoate mesogens

Soumya S. Patnaik[a]; Ruth Pachter[b]; Timothy J. Bunning[b]; Robert L. Crane[b]; W. Wade Adams[b]

[a] Department of Materials Science and Engineering, University of Virginia, Charlottesville, Virginia, U.S.A. [b] Wright Laboratory, Materials Directorate, Ohio, U.S.A.

PLEASE SCROLL DOWN FOR ARTICLE

A molecular simulation study of a cyclic siloxane with attached biphenylyl 4-allyloxybenzoate mesogens

by SOUMYA S. PATNAIK*†

Department of Materials Science and Engineering, University of Virginia,
Charlottesville, Virginia 22903, U.S.A.

RUTH PACHTER, TIMOTHY J. BUNNING, ROBERT L. CRANE
and W. WADE ADAMS

Wright Laboratory, Materials Directorate, WL/MLPJ Wright-Patterson AFB,
Ohio 45433, U.S.A.

A molecular simulation study of a cyclic siloxane macromolecule based on a pentamethylcyclosiloxane core and biphenylyl 4-allyloxybenzoate mesogenic units is reported. Molecular dynamics and semi-empirical calculations were used to provide insight into the conformation and the dielectric properties of the material. Out of three proposed conformations of the molecules, a cylindrical conformation was found to be the most probable. The intermolecular interactions were found to be optimized for the case where the mesogenic groups were planar and parallel to each other. The calculated mesogen length and inter-mesogen distances were consistent with available X-ray data. Electrostatic interactions were found to make a very significant contribution to the total energy. For the cylindrical model, the major component of the dipole was calculated to be along the long axis of the molecules. This is consistent with the alignment of the molecules parallel to a low frequency applied electric field as found experimentally.

1. Introduction

Recently we have been interested in understanding the structure–property relationships present in cyclic siloxane based liquid crystals [1–6] in an effort to develop these materials for optical applications. The cyclic siloxanes have been characterized using both X-ray and electron microscopy techniques and different packing schemes have been proposed to explain the observed packing behaviour [4, 5]. Atomistic simulation studies have also been reported [2, 3, 6], but a complete understanding of the role of the ring, the mesogenic groups and the spacer groups in determining the molecular structure and the liquid crystalline behaviour is still lacking. In liquid crystalline linear polysiloxanes with mesogenic side chains attached to the polysilane backbone by long spacers, the side chains are decoupled from the backbone and the molecular structure is primarily dictated by inter-mesogen interactions. It was expected that the presence of a small siloxane ring with mesogenic groups attached by short spacer groups might enforce intramolecular constraints that preclude certain kinds of inter-mesogen interactions, thereby making these cyclic siloxanes different from the linear polysiloxanes [5]. However, very little difference has been observed in the thermal transitions of these linear and cyclic siloxanes [4].

* Author for correspondence.
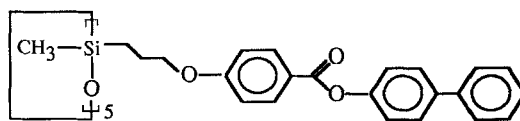† Mailing address is: WL/MLPJ, Bldg 651, 3005 P St., Ste 1, Wright-Patterson AFB, Ohio 45433-7702.

Figure 1. Structure of cyclic siloxane with pentamethylcyclosiloxane core and biphenylyl 4-allyloxybenzoate mesogen units.

We have carried out molecular simulations of a cyclic siloxane compound based on a pentamethylcyclosiloxane core and biphenylyl 4-allyloxybenzoate mesogens (BCS) (see figure 1) to complement our present understanding of the liquid crystalline siloxane system. BCS exists in a nematic phase above $\cong 120°C$ [7]. On application of an electric field at low frequency, the nematic samples exhibit multiple periodic meridional reflections on wide angle X-ray diffraction patterns [1] and the the molecular director aligns parallel to the applied electric field (perpendicular to the electrodes). On cooling below 110°C, the diffraction patterns of these samples show sharp Bragg reflections indicating the presence of partial crystallinity [7].

Liquid crystals have conventionally been simulated by representing the molecules as hard particles interacting by simple model potentials [8–12]. Although these methods have been very successful in explaining the broad features of the liquid crystalline phase, they do not provide a detailed insight. Such a study is even more relevant to our system where the mesogens are quite large and complex and therefore cannot be accurately represented by simple potentials. Furthermore, liquid crystals have a small stabilization energy, i.e. the enthalpy change associated with the liquid crystal–liquid phase transition is small. Thereby small changes in the molecular structure which in turn produce changes in molecular interactions can affect the phase structure significantly. Thus, any attempt realistically to predict properties and phase behaviour of liquid crystalline materials should take into account all possible molecular interactions, which can be done by atomistic calculations.

Molecular mechanics (MM) [13] and molecular dynamics (MD) [14] calculations, which provide an understanding of the molecular association and intermolecular interactions by a classical approach, have been used in this study. Although by using a classical approach, large molecular systems can be modelled and the method is computationally fast, the accuracy of MM is solely dependent on its parameterization scheme. Therefore, whenever possible, results from *ab initio* and semi-empirical quantum mechanical calculations on small model molecules were integrated with those from molecular dynamics calculations on BCS molecules to model the molecular system more accurately. The dielectric properties of the material were studied by calculating the dipole moment of the molecule using semi-empirical quantum mechanical methods. BCS shows strong alignment in an applied electric field [1] and the dipole moment was calculated for the most probable model found from MD simulations. Both the magnitude of the dipole and the direction of its major component were calculated.

It should be pointed out that although our main goal is to understand the liquid crystalline phase, all the MD simulations reported in this paper were carried out at room temperature where the material is crystalline. These initial studies were confined to room temperature because of the availability of X-ray crystallographic data. By comparing our results with the experimental data, we hope to be able to distinguish between probable molecular models. Subsequent simulations of the higher tempera-

ture nematic phase will be based on the room temperature structure; thus the room temperature study would help our understanding of the nematic phase and of this whole family of cyclic siloxane based liquid crystals.

2. Computational methods

2.1. Ab initio *calculations*

Ab initio calculations were carried out using GAUSSIAN 90 [15] for a geometry optimization of the siloxane ring. The 6–31G* basis set was applied. This is a split-valence polarization basis set $(10s, 4p, 1d)$ to describe a $(3s, 2p, 1d)$ configuration with six Gaussians combined to form the first s contraction, three to form the second s combination and the third being an uncontracted primitive. Similarly, three primitives are combined to form the first contracted p, while the second is uncontracted. Calculations were performed on a Cray X-MP using the 'direct' option in which the atomic orbital integrals are calculated as needed. This does not require internal storage, but involves additional computational effort. The calculated partial atomic charges of silicon and oxygen atoms are given in table 1.

2.2. *Semi-empirical calculations*

The calculations were carried out using MOPAC 6·0 [16], a semi-empirical molecular orbital package, and methods based on variants of the NDDO (neglect of diatomic differential overlap) approximation were used. In NDDO methods, all interactions except those arising from diatomic differential overlap are considered. Different hamiltonians such as MNDO (modified neglect of differential overlap), AM1 (Austin model 1) and PM3 (parametric method number 3) were applied.

2.3. *Molecular dynamics*

Molecular dynamics calculations were performed using the programs CHARMm and QUANTA [17]. MD represents molecules by an empirical force field and allows for the calculation of the kinetic energy of the system. It can therefore be used to study the dynamic properties of the molecules. All hydrogen atoms were modelled explicitly and a constant dielectric constant of 1·0 was used. The energies of the starting models were minimized by first using 100 cycles of Steepest Descent (to remove bad contacts) and then 2000 cycles of Adopted Basis Newton Raphson (a modified Newton Raphson

Table 1. Calculated partial atomic charges on the siloxane rings (in electrons).

Siloxane ring	Atom	MNDO	AM1	6–31G*
$(SiOH_2)_5$	Si	1·772	1·568	
	O	−1·000	−0·956	
$(HSiOCH_3)_5$†	Si	1·718	1·652	1·310
	O	−0·987	−0·960	−0·856
	C	−0·362	−0·653	0·802
$(CH_3SiOCH_3)_5$	Si	1·694	1·722	—
	O	−0·981	−0·962	—
	C	−0·347	−0·652	—

† The atomic charges are slightly different for the different relative orientations of the methyl and hydrogen groups in $(HSiOCH_3)_5$; therefore the numbers given in the table are an average.

technique especially suitable for macromolecules). Smoothing of the non-bonded interactions was done by using the 'switching' function for van der Waals interactions and the 'shifting' function for electrostatic interactions as implemented in CHARMm [18]. A 15 Å 'cut-off' distance for constructing the non-bonded list, a 14 Å 'cut-off' distance for the 'shifting' and the 'switching' functions and an 11 Å 'cut-on' distance for turning on the 'switching' functions were used. The simulations showed conservation of energy as would be expected for such large cut-off distances.

The minimized structure which represents the molecule with no kinetic energy, i.e., at 0 K was slowly heated to 300 K over 5 ps by randomly assigning velocities to each atom. The system was then equilibrated for 20 ps at this temperature by periodically scaling the velocities to maintain a constant average temperature. Once equilibrated, the molecular motion was traced by the simulation trajectory for 100 ps, during which the coordinates were saved every 100 steps. A time step of 0·001 ps was used which is reasonable with the use of SHAKE (used to constrain the high frequency bond stretching of hydrogen containing bonds).

3. Results and discussion

3.1. *Semi-empirical calculations*

Dipole moment calculations were carried out to investigate the dielectric properties of the molecule. The partial atomic charges used in the electrostatic term of the molecular mechanics force field are less reliable, because conformationally dependent charges are not taken into account. Therefore, instead of molecular mechanics, semi-empirical quantum mechanical methods based in the NDDO approximation were used. The BCS molecule consists of 250 atoms which cannot be handled by semi-empirical calculations [16], hence the dipole moments of the ring and mesogenic units were separately calculated. The calculations were carried out for a segment of the mesogen $(CH_3O-C_6H_4-COO-C_6H_4-C_6H_5)$ (shown in figure 2) and for three different ring systems, $(SiOH_2)_5$, $(HSiOCH_3)_5$ and $(CH_3SiOCH_3)_5$. The alkyl segment at the end of the original mesogen (biphenylyl 4-allyloxybenzoate) was not included, because it was not expected to have any significant contribution on the delocalization of the electron density of the other atoms (considered mainly responsible for the dipolar nature of the mesogen). Three different siloxane rings were considered in order to study the effect of different substituents on the conformation of the siloxane ring. The individual contributions from the mesogenic unit and the ring were added for the various conformations of the molecule to give the total dipole moment for a specific case. Different conformations of the molecule had to be considered, because the dipole moment depends on the conformation and the arrangements of the mesogenic groups relative to each other and is therefore biased towards a particular starting model.

The dipole of the siloxane ring depends both on the conformation of the ring and also on the partial charges on the constituent atoms. The calculated partial atomic charges vary depending on the semi-empirical method used. Therefore in order to estimate the variation in the partial atomic charges on the silicon and oxygen atoms in
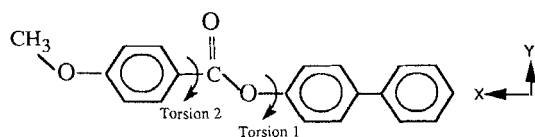

Figure 2.   The mesogen segment used for dipole calculations.

the siloxane ring, the corresponding atomic charges for optimized geometries of the various siloxane rings were calculated using MNDO and AM1 (see table 1). The AM1 hamiltonian was used because it has generally been found to be more reliable than MNDO or PM3 in calculating the dipole moment [19], while MNDO was applied to check the sensitivity of the partial atomic charges on the use of the different methods. The Natural population analysis based on the orthogonal atomic orbital approach [20] was used to partition the atomic charges. This technique may be more reliable than the Mulliken population (MP) analysis, which uses non orthogonal atomic orbitals (for example, the problem of negative orbital occupancy, which may be sometimes found for MP is believed to be eliminated when applying the Natural population analysis). The calculated atomic charges for the different conformations and methods used were found to be similar. No systematic differences were found between the MNDO and AM1 results (see table 1), although in most cases the atomic charges calculated by AM1 were smaller than those by MNDO. It is interesting to point out that the *ab initio* derived partial atomic charges are closer to the AM1 results. *Ab initio* calculations using the largest computationally reasonable basis set are currently underway to estimate better the partial atomic charges for different isomers of the siloxane rings [21].

The geometries of initial structures minimized by the molecular mechanics method (CHARMm force field) were further optimized and the dipole moments were calculated for the different rings, as shown in table 2. Relatively large differences were observed for all the three ring systems depending on the method used, but in all cases the maximum component of the dipole was found to be almost normal to the ring. As is expected, the dipole moment of $(HSiOCH_3)_5$ was found to be dependent on the relative orientation of the methyl groups (shown in table 2, when applying MNDO). For comparison, the dipole moment calculated using the CHARMm force field is also given. Since the electrostatic charges are not well parameterized in a molecular mechanics force field, the dipole moments are very different from those calculated using the semi-empirical methods.

As in the case of the siloxane ring, a large variation was found in the calculated dipole moment of the mesogenic segment (see table 3), depending on the method used. However, for all subsequent detailed calculations AM1 was used (AM1 has been found

Table 2. Calculated dipole moments of the siloxane rings (in Debye).

Siloxane ring	MNDO	AM1	QUANTA
$(SiOH_2)_5$	0·070	0·015	1·975
$(HSiOCH_3)_5$	0·374, 0·151, 0·238†	1·804	3·142
$(CH_3SiOCH_3)_5$	0·104	0·151	0·961

† The three different values are for three different relative orientations of the methyl units attached to the silicon atoms.

Table 3. Dipole moments and heats of formation of the mesogen segment using different methods.

	AM1	PM3	MINDO3	MINDO	QUANTA
Dipole moment/Debye	2·417	2·067	3·206	2·108	0·561
Heat of formation/kcal mol^{-1}	−32·62	−35·48	−54·15	−41·22	—

to be more reliable for dipole moment calculations [19]). Since it is apparent that the calculated dipole moment is dependent on the conformation of the mesogen segment, the changes in the dipole moment were investigated as a function of rotation about two torsion angles (as shown in figure 2). These two torsion angles were chosen because they were expected to make major contributions to the delocalization of the electron density of the constituent atoms.

The total dipole moment of the mesogen and its long axis component (component of the total dipole moment along the long axis of the mesogen) are shown in figures 3 and 4, respectively, as a function of the torsion angles. The maximum dipole moment of
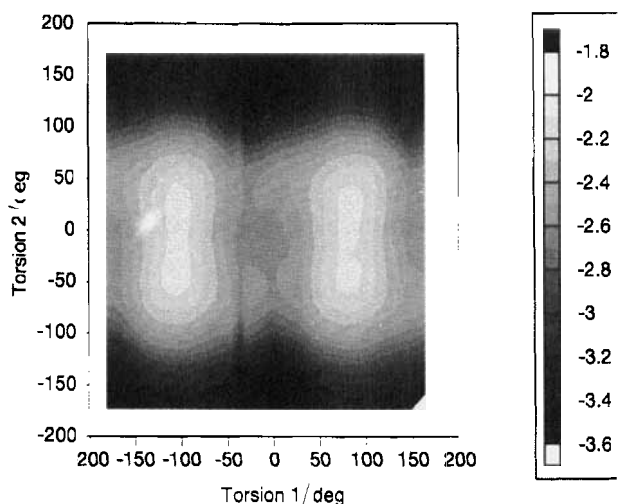
Figure 3. A contour map of the dipole moment of the mesogen segment calculated as a function of torsion angles 1 and 2. The grey scale in the legend corresponds to variation in the values of the dipole moment (in Debye) with the black colour representing maximum values.
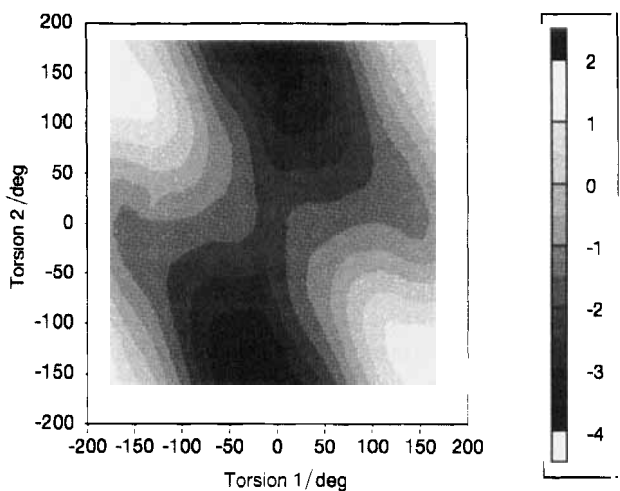
Figure 4. Long axis component of the dipole moment (in Debye) or the mesogen segment calculated as a function of torsion angles 1 and 2. The negative values in the legend correspond to the component along the $-x$ direction (x is defined in figure 2) and the darkest areas show maximum values.

the mesogen segment was found to be 3·4 D (for Torsion 2 equal to 180 and Torsion 1 eqal to 0 deg). The long axis component of the dipole was also found to be a maximum for the same conformation. These results show that for coplanar segments, the total dipole moment is a maximum and the major component of the dipole is along the long axis of the mesogen segment. Since the dipole moment of the mesogen is much larger than that of the ring, the mesogen units seem to be mainly responsible for the dipolar characteristic of the molecule. As described later in the molecular dynamics section, a cylindrical model was found to be the most probable conformation. Since the major component of the dipole of the ring was found to be along the normal to the ring, for a cylindrical model (see figure 7(a)) the contributions from the ring and the mesogen units add up along the long axis of the molecule and the major component of the dipole is along that direction. This is consistent with the observed dielectric response of the material at low temperatures and frequencies, when the molecules align parallel to the applied electric field [1]. However, it is important to point out that the electrostatic interactions are not necessarily solely responsible for the dielectric response of this family of LC materials and that the steric interactions which contribute to the viscosity of the material may also make a significant contribution. Other mesogens with comparable calculated dipole moments have been found not to align very well in an electric field.

In order to find low energy conformations of the mesogen units and to compare them to the coplanar structure (which was found to be favoured by the MD simulations), the heat of formation was calculated as a function of Torsions 1 and 2. A contour map of the heat of formation calculated at 15 deg increments is shown in figure 5. For clarity of representation, all values of heat of formation which were less than 30 kcal mol^{-1} are not shown in the plot. The coplanar conformation was not found to be of lowest energy and minimum values were found for Torsion 2 equal to zero and Torsion 1 equal to ± 50 deg. Figure 6 shows the variation in the heat of formation as a function of Torsion 1, with Torsion 2 fixed at the planar conformation. The difference between the maximum heat of formation (Torsion 1 = 0 deg) and the minimum heat of formation (Torsion 1 = 0 deg) and the minimum heat of formation (Torsion 1 = 50 deg)
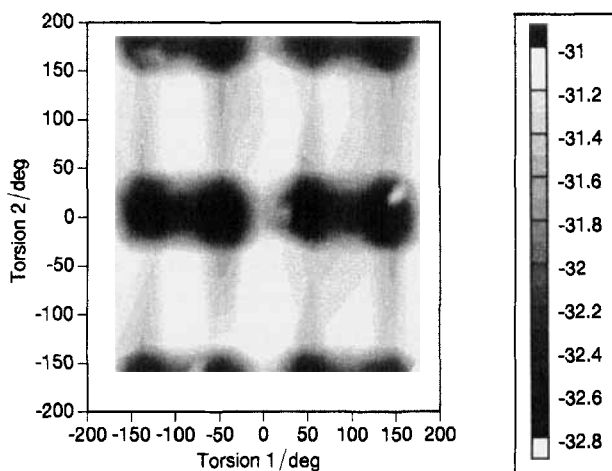

Figure 5. Calculated heat of formation (in kcal mol^{-1}) of the mesogen segment as a function of torsion angles 1 and 2. The dark regions represent areas with low heat of formation.
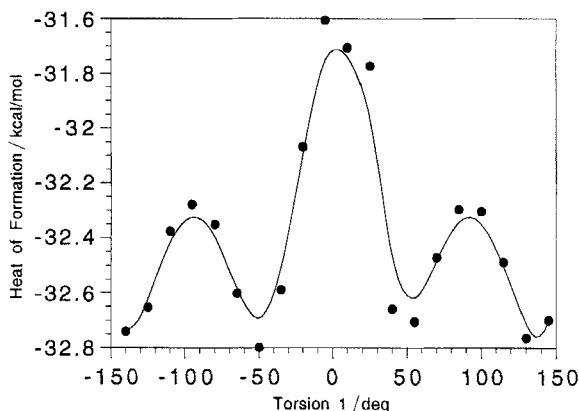
Figure 6. Calculated heat of formation of the mesogen segment as a function of Torsion 1 with Torsion 2 fixed at planar conformation.

was calculated to be about $1.2 \, \text{kcal} \, \text{mol}^{-1}$. It should be pointed out that these calculations were carried out on single mesogenic segments and unlike the MD simulations, where the intermesogen interactions were taken into account, in the present case those interactions were ignored.

3.2. *Molecular dynamics simulations*

Two different models, a cylindrical model (the shape of the molecule resembling a rod), and a disk-like model (the shape resembling a disk), can be envisaged on the basis of the chemical structure of BCS [5]. The minimized energies of the cylindrical and the disk-like conformations are summarized in table 4. Although the minimized energy (see table 4) of the cylindrical model was found to be lower than that for the disk-like model, some initial MD simulations were carried out on both models for a more definite distinction.

Results from MD simulations carried out on isolated disk-like molecules indicated that, during the simulation, the disk-like model changes towards a cylindrical conformation. This suggests weak coupling between the core and the rigid mesogen units, thereby making the cylindrical model more probable. Both in the case of the cylindrical and the disk-like conformations, the siloxane ring was found to be very flexible with a large range of available torsion angles (shown in figure 7 (a) for the cylindrical model) giving rise to various possible conformations. The flexibility of the ring and the nature of the spacer groups could be responsible for the weak coupling between the core and the mesogen units, and the cylindrical model was used for all subsequent simulations.

Since the electrostatic interactions were found to make a relatively large contribution to the total energy of the molecules (see table 4), MD simulations on the cylindrical model with and without electrostatic interactions were performed. When the electrostatic interactions in the force field were neglected, it was found that a conical structure evolved with the five mesogen units getting closer (see figure 8 (a)). A conical model has earlier been proposed as a probable conformation [5], and therefore in order to compare the conical model with that of our starting cylindrical model, the energy of the conical structure was minimized. The minimization was carried out both with and without electrostatic charges and it was found that although the conical model had lower energy than the cylindrical model when electrostatic charges were ignored, on

Table 4. Minimized energies for various models of the BCS molecule.

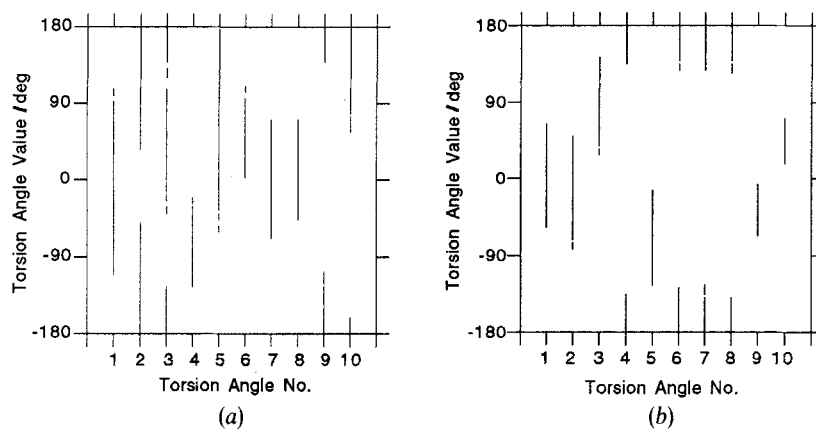| Energy/kcal mol^{-1}	Cylinder model	Disk-like model	Cone model
Total	−66·7	−33·0	−61·0
Bond	5·6	5·5	6·0
Angle	25·9	28·9	31·9
Dihedral	53·2	33·9	60·3
Improper	1·0	0·2	4·2
Lennard-Jones	−36·5	−8·9	−54·4
Electrostatic	−115·9	−92·2	−108·9

Figure 7. Range of torsion angles found during a 100 ps MD simulation at 300 K for all the 10 different torsion angles defining the siloxane ring: (*a*) without and (*b*) with the application of periodic boundary conditions.

including the electrostatic charges, the cylindrical model was found to be of lower energy (see table 4). The crowding of the mesogen units show that when electrostatic charges are neglected, the structural details are driven by interactions between the mesogenic groups and the ring is merely providing an anchoring effect. The strong interaction between the mesogen units was further demonstrated by simulation results on two molecules interdigitated along the long axis, with an initial ring separation distance of 27 Å. During the course of a 100 ps simulation, the separation distance between the interdigitated mesogen units became smaller and the ring separation distance decreased to 22 Å.

On inclusion of electrostatic interactions in the force field, the lowest energy conformation during the MD simulation was found to be a splayed structure (see figure 8 (*c*)). A 125 ps dynamics trajectory found the separation distance between the ester group in the mesogenic moiety and the siloxane ring decreasing. The interatomic distances (O–S) between the carbonyl oxygen atom in the ester group and its closest silicon atom in the siloxane ring were monitored during the simulation. It was observed that in all five cases (for the five mesogen units), the separation distances (O–S), which were different at the beginning of the simulation, decreased and levelled off during the simulation. It is interesting to note that they all levelled off at the same value (6·5 Å), and after about the same number of time steps (20 ps). As shown in figure 9, the dipole moment and the potential energy also decreased and levelled off after about the same
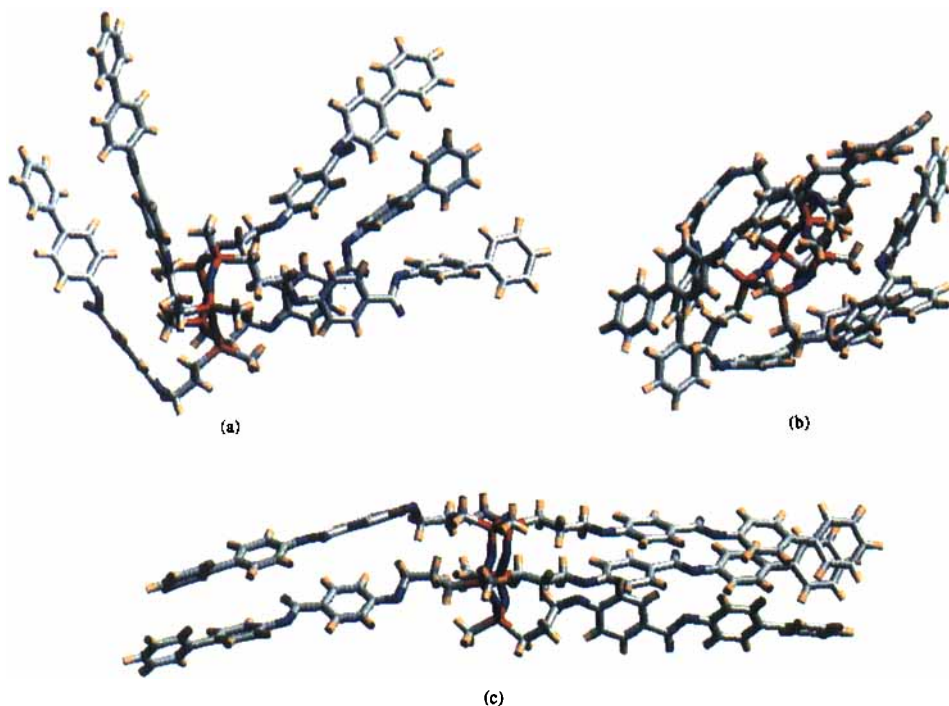
Figure 8. The different conformations of the BCS molecule. Silicon atoms are shown in red, oxygen in blue, carbon in grey and hydrogen in light brown. (*a*) conical; (*d*) splayed; (*c*) cylindrical.
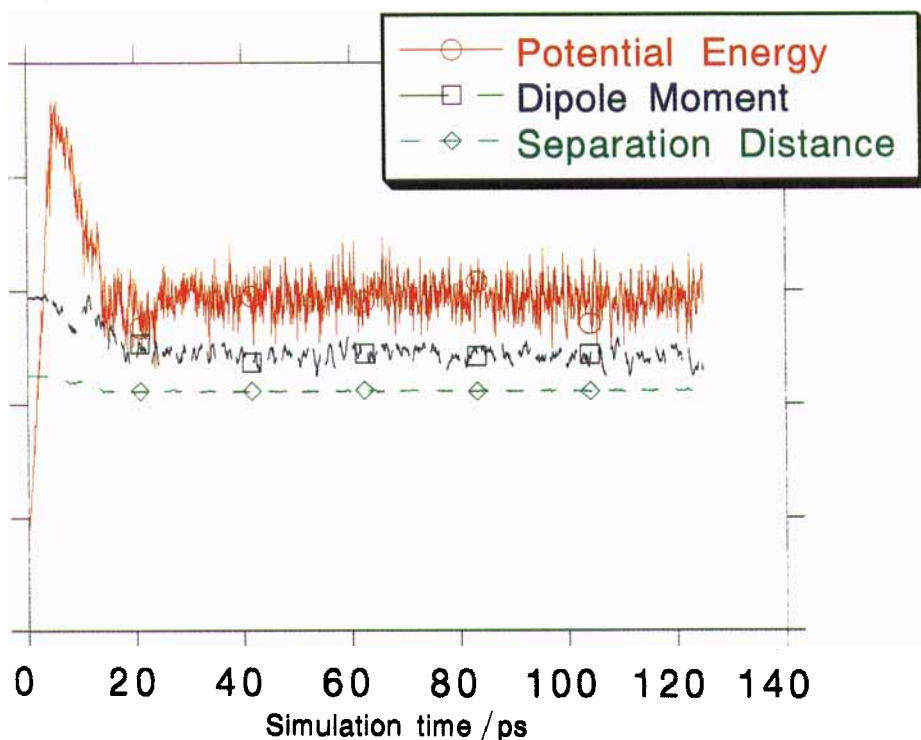

Figure 9. Molecular dynamics simulations at 300 K carried on a single BCS molecule with electrostatic interactions included in the force field. The separation distance is the interatomic distance between the carbonyl oxygen atom in the ether group of the mesogen unit and its closest silicon atom in the siloxane ring.

length of simulation time. The fact that the separation distance (O–S), the dipole moment, and the potential energy all achieved constant values after the same length of simulation time is significant and implies that the interaction between the ester group and the siloxane ring has direct influence on the potential energy and the dipole moment of the molecule.

These results indicate that the electrostatic interactions are significant and the evolution of the splayed structure is a direct result of the competition between the van der Waals interactions between the mesogenic groups and the electrostatic interactions between the polar groups (the ester group and the siloxane ring). Our simulations of the dynamics trajectory with and without electrostatic interactions clearly show that very different conformations can be observed, depending on the force field used and that for any realistic modelling, correct partial atomic charges should be utilized.

Since the anisotropy in the intermolecular interactions is mainly responsible for the formation of liquid crystalline phases, these interactions should be taken into account while modelling such systems. After carrying out some initial molecular dynamics simulations on isolated single molecules (in vacuum), we did subsequent simulations using periodic boundary conditions [17]. Only the coordinates of the primary structure were stored and the images (in our case, 26 images were used to generate a three-dimensional lattice) were generated by using transformation matrices. The primary system and its images were then used as a single molecular system. Most of the previously reported molecular dynamics simulations which take intermolecular interactions into account have been carried out either using a mean field approach or by generating a static lattice shell around the dynamic molecule. We did not use the mean field approach, because it does not provide detailed structural information, while the application of periodic boundary conditions is more suitable than using a static lattice shell, because, in our case, the images are allowed to change as the primary structure varies. Furthermore, the present method is computationally less extensive, because the image/image energy terms do not have to be evaluated.

For subsequent simulations, single molecules with periodic boundary conditions were considered. Since these MD simulations were carried out at room temperature, where the material is partially crystalline, whenever possible the periodic boundary conditions were based on available X-ray data [7]. A c repeat (along the long axis) distance of 27 Å was used, but due to the lack of sharp off-meridional reflections, no lateral intermolecular packing distances could be ascertained. In the absence of any experimental results for lateral packing, the a and b dimensions of the periodic boundary were taken to be equal to the distance corresponding to the minimum energy between two molecules as determined by Lennard-Jones and electrostatic energy potentials. The effect of using different periodic boundary conditions was investigated by considering three different types of lattice, rectangular ($a = b \neq c$, $\alpha = \beta = \gamma = 90°$), orthorhombic ($a \neq b \neq c$, $\alpha = \beta = \gamma = 90°$) and hexagonal ($a = b \neq c$, $\alpha = 120°$, $\beta = \gamma = 90°$), MD simulation results revealed no significant difference in the values of any of the variables and the energies of the lowest energy conformations were comparable in all three cases. A comparison of these molecular dynamics simulations with those performed on isolated single molecule shows that the boundary effects were clearly minimized. Also, unlike the case for isolated single molecule where the low energy conformations were different from the initial cylindrical model, on using the boundary conditions the initial cylindrical shape was preserved. Figure 8 (*a*) shows the lowest energy conformation for the cylindrical model with periodic boundary conditions during a 100 ps simulation.
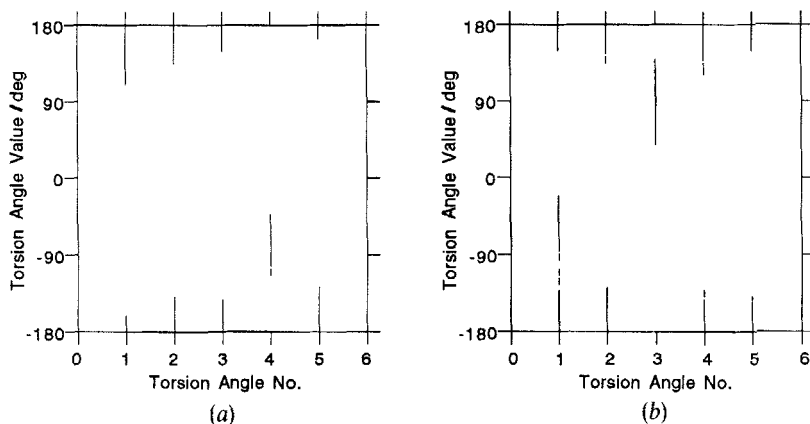
Figure 10.   Range of torsion angles about two bonds in the alkyl spacers found during a 100 ps
   MD simulation at 300 K with boundary conditions. (*a*) The $Si-C_1-C_2-C_3$ torsion for all
   the five mesogen units. (*b*) $C_1-C_2-C_3-O$ torsion for all the five mesogen units.

As in the case for modelling the molecule in vacuum, a large range of possible torsion angles was found for the torsion angles defining the ring (see figure 7 (*b*)), again indicating that the ring is very flexible. Mostly all-*trans*-bonds were found for the torsion angles in the alkyl spacers (see figure 10), implying that the spacers are fully extended. A large range of torsion angles about the biphenyl bond was calculated showing a low torsional energy barrier about this bond. The average structure shows the mesogen units to be almost planar and parallel to each other. The average inter-mesogen distance calculated for all the lowest energy structures of the dynamics run from the three different kinds of boundary conditions is about 5 Å. This is consistent with the average mesogen spacing of 5 Å which is found for a wide variety of liquid crystals [22]. The average mesogen length was found to be 23 Å, also consistent with our earlier model [7].

4.   Conclusions

Semi-empirical calculations shows that the dipole moment of the mesogen unit is a maximum for coplanar mesogen segments. The maximum component of the dipole of the siloxane ring is normal to the ring and therefore for a cylindrical model the major component of the dipole of the molecule is along its long axis. This supports the alignment [1] of the molecules parallel to the field at low frequency (effectively DC field). Although the steric interactions favour both parallel or anti-parallel packing of mesogens [23], the electrostatic interactions could be responsible for the interdigitated structure, because the dipoles of the mesogen units would favour an anti-parallel packing. The results from the semi-empirical calculation, in conjunction with those from the MD simulations, which favours the packing of coplanar mesogens, explain the good alignment of the molecules in electric fields.

The molecular dynamics results indicate that the cylindrical conformation is a more probable conformation for BCS, and the intermolecular interactions are optimized for the case where the mesogen units are almost planar and parallel to each other. It is interesting to point out that although the presence of the siloxane ring (which is very flexible) does not produce a more rigid molecule, the ring acts as more than just an anchor to the mesogen units, since the electrostatic interaction between the ring and the ester group in the mesogen segment also affects the molecular conformation.

The simulations done in the present study have been done on single molecular systems. However, cooperative behaviour of the molecules, i.e. dipole–dipole and orientational correlation (which are very significant for liquid crystals) can only be studied for a cluster of molecules. Calculations are presently underway on a three-dimensional cluster of 27 molecules using a parallelized version of CHARMm [21].

References

[1] BUNNING, T. J., McNAMEE, S. G., McHUGH, C. M., PATNAIK, S. S., OBER, C. K., and ADAMS, W. W., 1993, *Materials Research Society Symposium Proceedings*, Vol. 307 (Materials Research Society), p. 311.

[2] PACHTER, R., BUNNING, T. J., CRANE, R. L., ADAMS, W. W., SOCCI, E. P., and FARMER, B. L., 1993, *Makromolek. Chem. Theory Simul.*, **2**, 337.

[3] SOCCI, E. P., PACHTER, R., BUNNING, T. J., FARMER, B. L., and ADAMS, W. W., 1993, *Liq. Crystals*, **13**, 811.

[4] BUNNING, T. J., KLEI, H. E., SAMULSKI, E. T., CRANE, R. L., and ADAMS, W. W., 1993, *Molec. Crystals liq. Crystals*, **231**, 163.

[5] BUNNING, T. J., KLEI, H. E., SAMULSKI, E. T., CRANE, R. L., and LINVILLE, R. J., 1991, *Liq. Crystals*, **10**, 445.

[6] PACHTER, R., BUNNING, T. J., and ADAMS, W. W., 1991, *Comput. Polym. Sci.*, **1**, 179.

[7] BUNNING, T. J., 1992, Ph.D. Dissertation, University of Connecticut.

[8] ALLEN, M. P., FRENKEL, D., and TALBOT, J., 1989, *Comput. Phys. Rep.*, **9**, 301.

[9] ALLEN, M. P., and WILSON, M. R., 1989, *J. Comput.-Aided Molec. Des.*, **3**, 335.

[10] ALLEN, M. P., 1990, *Phys. Rev. Lett.*, **65**, 2881.

[11] FRENKEL, D., 1992, *Phase Transitions in Liquid Crystals* (Plenum Press), p. 67.

[12] HASHIM, R., LUCKHURST, G. R., and ROMANO, S., 1985, *Molec. Phys.*, **56**, 1217.

[13] BURKERT, U., and ALLINGER, N. L., 1982, *Molecular Mechanics* (ACS Monograph, edited by M. C. Caserio, Vol. 177), (American Chemical Society).

[14] McCAMMON, J. A., and HARVEY, S. C., 1987, *Dynamics of Proteins and Nucleic Acids*, (Cambridge University Press), p. 35.

[15] Gaussian is a connected system of programs for performing semi-empirical and *ab initio* molecular orbital calculations. Gaussian 90 was developed in 1990 by Firsch, M. J., Head-Gordon, M., Trucks, G. W., Foresman, J. B., Schlegel, H. B., Raghavachari, K., Robb, M. A., Binkley, J. S., Gonzalez, C., Defrees, D. J., Fox, D. J., Whiteside, R. A., Seeger, R., Melius, C. F., Baker, J., Martin, L. R., Stewart, J. J. P., Topiol, S., and Pople, J. A. It is available from Gaussian, Inc.m Pittsburgh, PA.

[16] MOPAC is a general purpose semi-empirical molecular orbital package developed by J. J. P. Stewart. It is available from QCPE at Indiana University, Department of Chemistry, Bloomington, IN.

[17] QUANTA is a molecular modelling package developed by Molecular Simulation Inc., Waltham, MA 02154.

[18] BROOKS, B. R., BRUCCOLERI, R. E., OLAFSON, B. D., STATES, D. J., SWAMINATHAN, S., and KARPLUS, M., 1983, *J. Comput. Chem.*, **4**, 187.

[19] STEWART, J. J. P., 1990, *Reviews in Computational Chemistry* (VCH Publishers Inc.), p. 72.

[20] REED, A. E., WEINSTOCK, R. B., and WEINHOLD, F., 1985, *J. chem. Phys.*, **83**, 735.

[21] PATNAIK, S. S., PACHTER, R., CRANE, R. L., and ADAMS, W. W., in preparation.

[22] LEADBETTER, A. J., 1979, *The Molecular Physics of Liquid Crystals*, edited by G. R. Luckhurst and G. W. Gray (Academic Press), p. 299.

[23] SOCCI, E. P., 1993, M.S. Thesis, University of Virginia.